Journal of Integrative Neuroscience, Vol. 2, No. 1 (2003) 31–44

Imperial College Press
www.icpress.co.uk

TWO SPECIES OF GAMMA OSCILLATIONS IN THE OLFACTORY BULB: DEPENDENCE ON BEHAVIORAL STATE AND SYNAPTIC INTERACTIONS

LESLIE M. KAY

Department of Psychology, Institute for Mind & Biology, University of Chicago, 940 E. 57th Street, Chicago, IL 60637, USA
LKay@uchicago.edu

Received 1 March 2003
Revised 25 March 2003

Gamma oscillations (40–100 Hz), originally seen in the olfactory bulb (OB), have long been a defining characteristic of sensory coding in the olfactory system. This study proposes that gamma oscillations are of two types, associated with different behavioral features and synaptic origins within the OB. Local field potentials were recorded from rat and mouse OBs during various behavioral periods (immobility, alert motionlessness, exploration and odor discrimination). High frequency gamma activity (65–100 Hz) is shown to be correlated with the sniff cycle, initiated at the peak of inhalation and is called type 1 gamma. It is prominent during exploratory behavior, but also present during resting and trained odor discrimination. Low frequency gamma activity (35–65 Hz), called type 2 gamma, is not strongly correlated with the sniff cycle, is inhibited by the sniff onset and is prominent during alert immobility. Rest and alert immobility are characterized by alternating type 1 and type 2 gamma rhythms, while exploratory sniffing and odor discrimination show a dramatic decrease in type 2 gamma with a broadband increase in the power of type 1 gamma. Periods of alert immobility prior to odor discrimination in trained animals show dominance of type 2 gamma, with episodes lasting up to 0.5 second. Data from mice with selective deletion of granule cell inhibition in the OB show a selective loss of type 2 gamma with type 1 gamma dramatically enhanced during exploratory behavior, suggesting that mutual inhibition between granule cells or centrifugal inhibitory input drives type 2 gamma, and that the excitatory-inhibitory connections between mitral and granule cells likely drive type 1 gamma. Gamma activity is not a single type of oscillation, and the largest amplitude gamma bursts are often those associated with an attentive cognitive state rather than odor sniffing.

Keywords: Gamma oscillations; mutual inhibition; olfactory bulb; theta oscillations; granule cells; local field potential; coupled oscillator; behavior.

1. Introduction

Olfactory bulb (OB) odor-evoked oscillations of approximately 40–50 Hz were described by Adrian [1] elicited in hedgehogs under anesthesia upon the inhalation of amyl acetate. Since that time, these oscillations, dubbed "gamma" by Bressler and Freeman [5], have been seen in the OB and piriform cortex (PC) of waking

animals and have been the focus of many computational models describing odor processing in the OB [11, 14, 27, 28]. Similar odor-evoked oscillations at lower frequencies (20 Hz) have also been seen in insects and fish [17, 25] and have been linked to odor coding and discrimination [3, 34, 35]. Outside of the olfactory system gamma oscillations have been noted in the visual and motor systems [8, 10, 18, 29–31] and the hippocampus [6, 7, 26]. They have been linked to sensory coding, memory consolidation and attention.

In mammalian olfactory studies the term "gamma" has been used to refer to oscillations in the range of 40 to approximately 100 Hz, with the frequency range dependent on the species and presence or absence of anesthesia. Gamma activity has been described as a single wide frequency band and individual oscillations associated primarily with inhalation and olfactory bulb theta rhythm [12, 23]. In this study I argue that there are in fact two types of gamma oscillations with different relationships to the OB theta rhythm and behavioral state. Examination of data from genetically altered mice suggests that these two types of gamma activity have different synaptic origins in the OB.

2. Methods

2.1. *Animals, surgery and behavior*

Six adult male Sprague–Dawley rats (450 gm) were used. Five were implanted with stainless steel bipolar electrodes (1–2 mm tip separation) in the OB, anterior piriform cortex (PC), entorhinal cortex and the hilus of the dentate gyrus of the hippocampus and one with electrodes in the OB and anterior and posterior PC. After recovery, four rats were trained in an operant task, described in detail elsewhere [22]. The task required the animals to refrain from pressing a reward lever for a one second period in each trial (3–4 second marks in 6 second trials delivered with a 12 second intertrial interval). During this time a 3 second odor stimulus began and arrived at the sniffing port (3.5 second mark in 6 second trials). Pressing the lever after the 4 second mark in response to the CS+ resulted in delivery of one drop of sugar water, while pressing for the CS− or odorless control stimulus had no effect. Recording sessions consisted of 100 to 200 trials, approximately 2/3 CS+ trials, 1/3 CS− and 1/3 odorless control trials pseudorandomly intermixed. Odors were artificial orange and almond.

Two rats were recorded from during spontaneous behavior. Odors (isoamyl acetate, benzaldehyde, methyl salicylate and citronellal) were delivered on cotton swabs placed near the animal's nose or in the cage.

Knockout mice were bred at UCLA from donor animals and have been characterized in earlier studies [20, 32]. Deletion of the $\beta 3$ subunit of the $GABA_A$ receptor selectively disables granule cell receptors in the OB, while the mitral cell $GABA_A$ receptors remain functional. Seven mice ($3\beta 3-/-$ and $4\beta 3+/+$ controls) were implanted with stainless steel bipolar electrodes in the OB and after recovery were recorded from while spontaneous behavior was observed.

2.2. *Data collection*

Rats and mice were put in a box similar to the home cage or a modified home cage (for behavioral experiments) and data were recorded via a multichannel headstage (built in house for mice, NB Labs and Neuralynx HS-27 for rats). Local field potentials were digitized at 1 kHz or 2 kHz, with analog filters set at 1–300 Hz, 1–200 Hz or 1–475 Hz in different experiments. Data were examined offline to discard periods with movement or other artifacts. A Logitech Webcam Pro 3000 was used for video recordings of spontaneous behavior in rats.

2.3. *Data analysis*

Data were digitally filtered using Igor Filter Design Laboratory to produce noncausal filters in the broad gamma (35–115 Hz), low gamma (35–65 Hz) and high gamma (65–115 Hz) bands. Narrower filters were used to determine the demarcation for the high and low gamma bands. These were 20 Hz bands stepped by 5 Hz from 35–55 Hz to 95–115 Hz. High and low gamma band filtered data were smoothed using the RMS amplitude in stepped windows of 50 msec with a 1 point step, producing new time series of the RMS amplitudes. Cross correlations were performed between the theta rhythm and these smoothed gamma series to examine the amplitude and position of the peak correlation. Because it was only of interest to examine the correlation of time of occurrence between gamma activity and the inhalation, with the amplitudes of the signals being relatively meaningless to this question, data were normalized to zero mean and unit standard deviation after smoothing and before correlation.

Power spectra were calculated for individual data segments, using half-overlapping 128–1024 msec windows, depending on the length of continuous data segments. For behavioral trials, one-half second windows, chosen from the prestimulus and odor discrimination periods, were examined over 25–30 trials per animal. For spontaneous behavior (mouse power spectra), continuous periods of 7 to 41 seconds were used to estimate power spectra and the spectra were normalized by setting the power of the first theta peak during immobility for each animal to 1. Error bars on Fig. 1(b) were estimated using jackknife statistics across the data set [33].

3. Results

Observation of OB and PC data shows prominent gamma oscillations of two types [Fig. 1(a)]. Higher frequency gamma oscillations (70–90 Hz) appear on the peaks of OB theta waves associated with inhalation. Occasional lower frequency oscillations (50–60 Hz) are seen either in between sniffs or independent of the sniff cycle, sometimes spanning up to half a second. These lower frequency oscillations are large, occuring almost exclusively during immobility, and are most reliably present in animals during the alert waiting condition in behavioral trials. They are rarely if ever seen during active exploration or sniffing. Power spectra from different behavioral epochs confirm the difference in gamma band activity between these behavioral states [Fig. 1(b)].

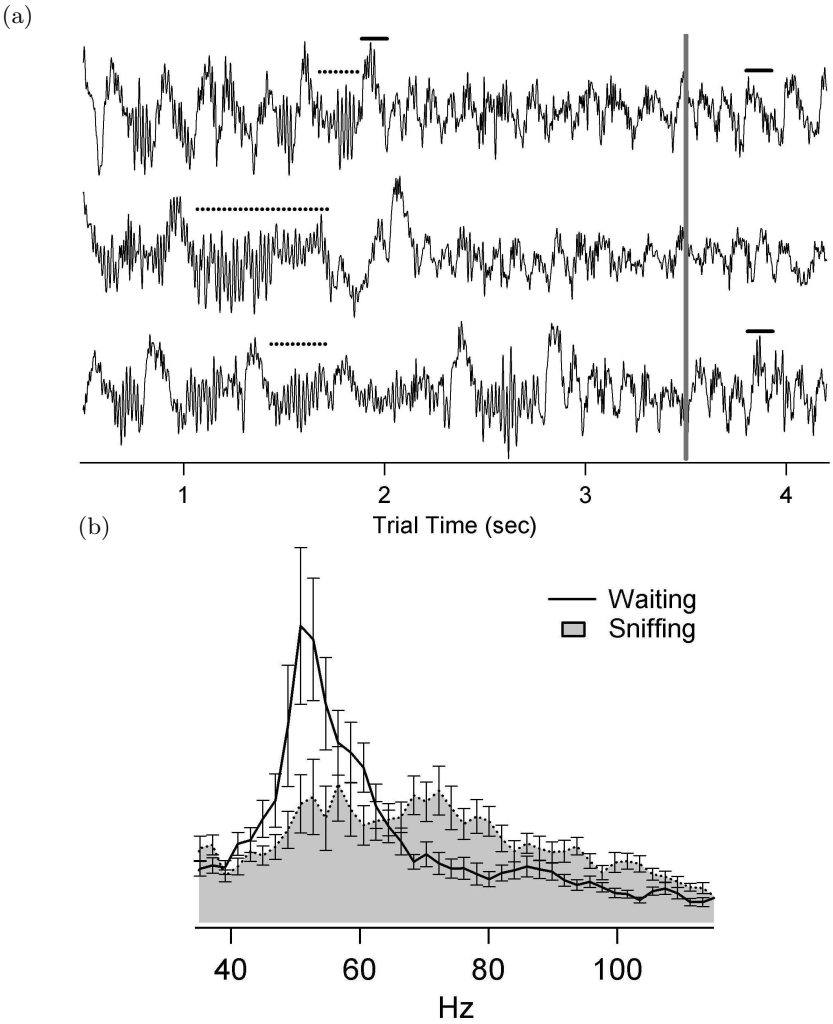

Fig. 1. Low and high frequency gamma oscillations. Data are from rat OB during execution of operant behavior. (a) Raw data from three representative trials show prominent low frequency gamma bursts (dashed overbar) during the waiting period before the odor stimulus begins. The vertical gray bar indicates odor onset, and the animal was required to refrain from pressing the response lever between the 3 and 4 second marks. Irregular high frequency bursts are indicated by solid overbars. (b) Power spectra estimated from 57 CS+ trials from one experiment. The early period ("waiting") was 1.5–2.0 seconds and the odor sniffing period was 3.5–4.0 seconds. Error bars indicate jackknifed error estimates, similar to standard deviation (see methods).

To determine the frequency ranges of the two types of gamma oscillations, data were digitally filtered in stepped 20 Hz pass bands (35–55 Hz, 40–60 Hz, etc.). After filtering, data were smoothed using the RMS amplitude, and the smoothed data were normalized (zero mean and unit standard deviation) and correlated with the normalized theta rhythm from the same epochs to determine whether the occurrence of gamma bursts was correlated with the sniff cycle [Fig. 2(a)]. Examination of data from periods of immobility or alert waiting shows a change at approximately

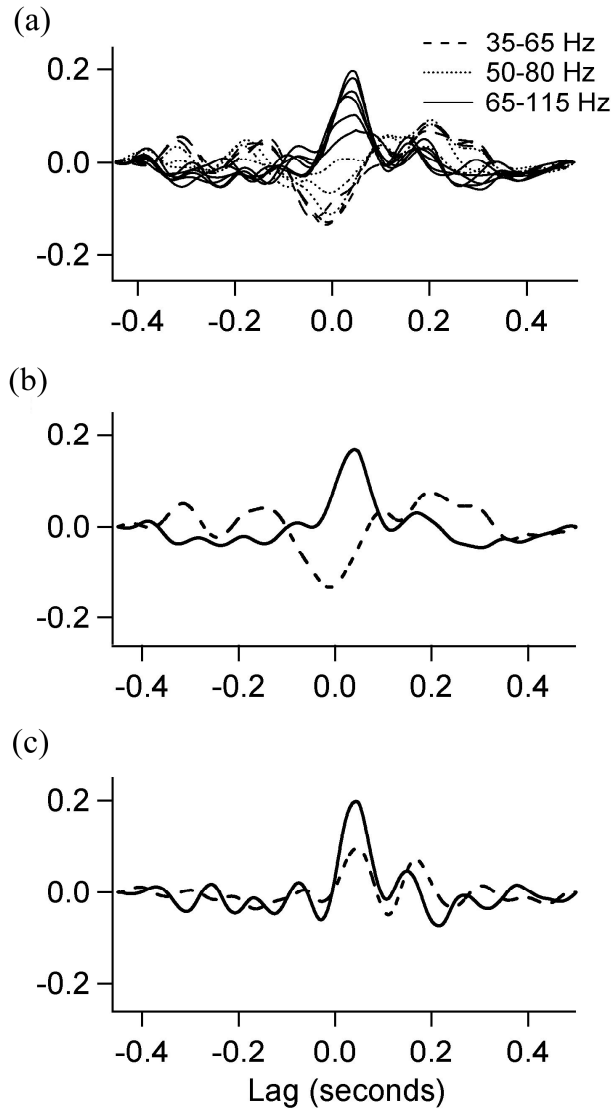

Fig. 2. Correlation estimates from data displayed in Fig. 1. (a) Data from the prestimulus waiting period were filtered in 20 Hz pass bands, stepped by 5 Hz from 35–55 Hz to 95–115 Hz. The resultant time series were smoothed, normalized and correlated with the normalized theta rhythm. Low gamma (coarse dashed line) has a different relationship with the theta inhalation cycle than high frequency gamma activity (smooth line). Filter bands that span the 65 Hz point (fine dotted line) show a correlation pattern midway between the two. (b) Combined high frequency and low frequency gamma-theta correlations during prestimulus waiting. (c) Gamma-theta correlations during active odor discrimination.

65 Hz. Activity in pass bands that span frequencies of 70–100 Hz shows significant correlation with the theta rhythm, with the peak of correlation near the peak of the theta rhythm [Fig. 2(b)]. Activity in pass bands that span frequencies of 40–65 Hz shows low, insignificant or negative correlation with the theta rhythm (degree

of correlation variable across animals and behavioral states), and the peak of this correlation is prior to the peak of inhalation [Fig. 2(b)]. Activity in pass bands that span the 65 Hz mark shows intermediate patterns suggesting summation of the two phenomena [Fig. 2(a)]. During the prestimulus alert waiting period, lower frequency gamma activity is prominent, as seen in the power spectrum [Fig. 1(b)]. Data from animals engaged in odor discrimination show preserved correlation with the theta rhythm for high frequency gamma activity while the low frequency activity

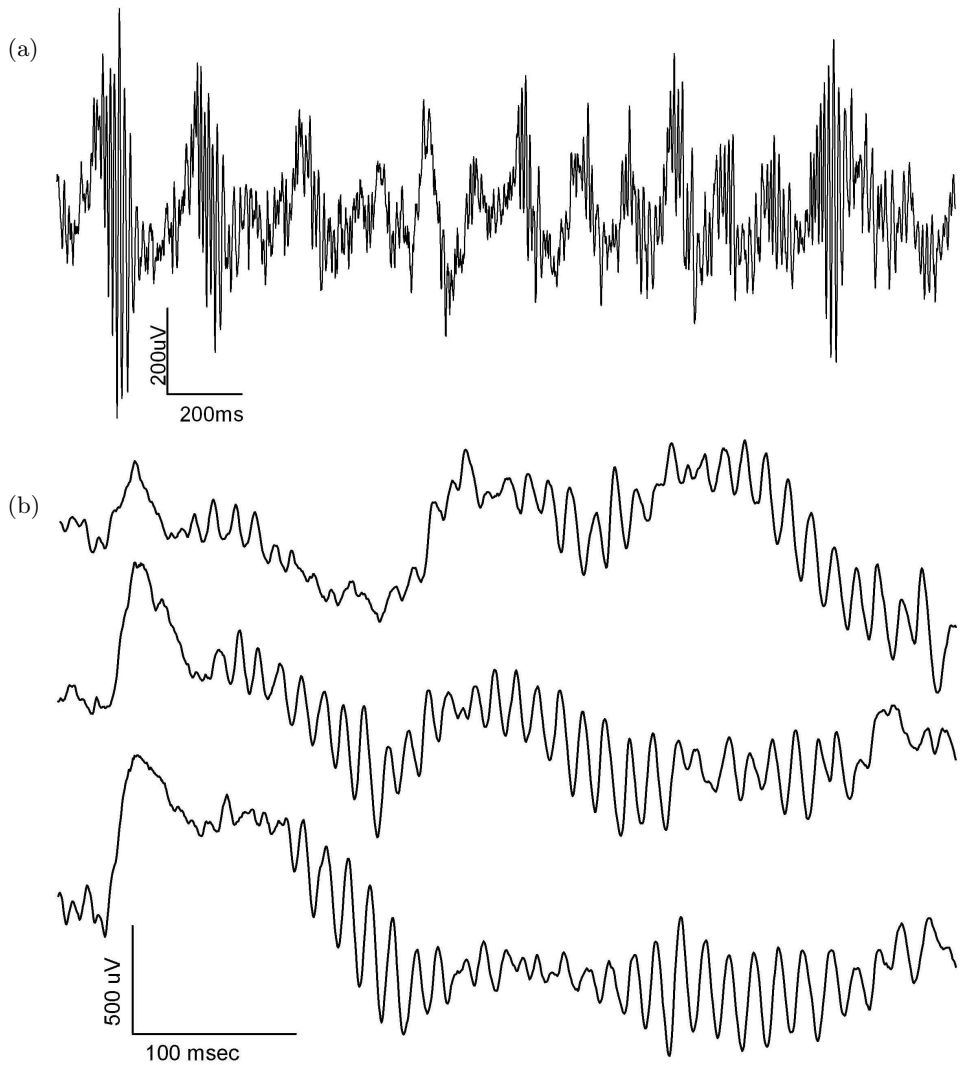

Fig. 3. Sniff- and odor-associated high frequency gamma bursts in rat OB during spontaneous behavior. (a) Fast sniffing with prominent high frequency gamma bursts (70–80 Hz) during exploration. (b) Odor-evoked potentials followed by 70 Hz oscillations. These were elicited by placing a swab of amyl acetate near the rat's nose and are also evident, although lower in power, when the swab is further away.

has a similar phase relationship to the theta rhythm [Fig. 2(c)]. Also during these periods, power spectra show a significant decrease in the lower frequency peak and an increase in broadband higher frequency gamma activity [Fig. 1(b)].

While high frequency gamma activity is observed during odor sniffing in trained rats, it is relatively irregular compared with the low frequency bursts seen during alert motionlessness [Fig. 1(a)]. However, when untrained rats are allowed to explore an unfamiliar environment, high sniffing rates are seen and the high frequency gamma bursts (70–80 Hz) resemble the classic picture, with onset near the peak of the theta rhythm [Fig. 3(a)]. When presented with a relatively strong but non-aversive novel odor on a swab, a distinct evoked potential is seen, followed by prolonged high frequency odor-evoked gamma oscillations [Fig. 3(b)].

$\beta 3 -/-$ mice have a deletion of the $\beta 3$ subunit of the $GABA_A$ receptor [20]. In the OB, this selectively disables granule cell $GABA_A$ receptors, leaving mitral cell $GABA_A$ receptors intact [32]. Control mice ($\beta 3 +/+$) show gamma and theta

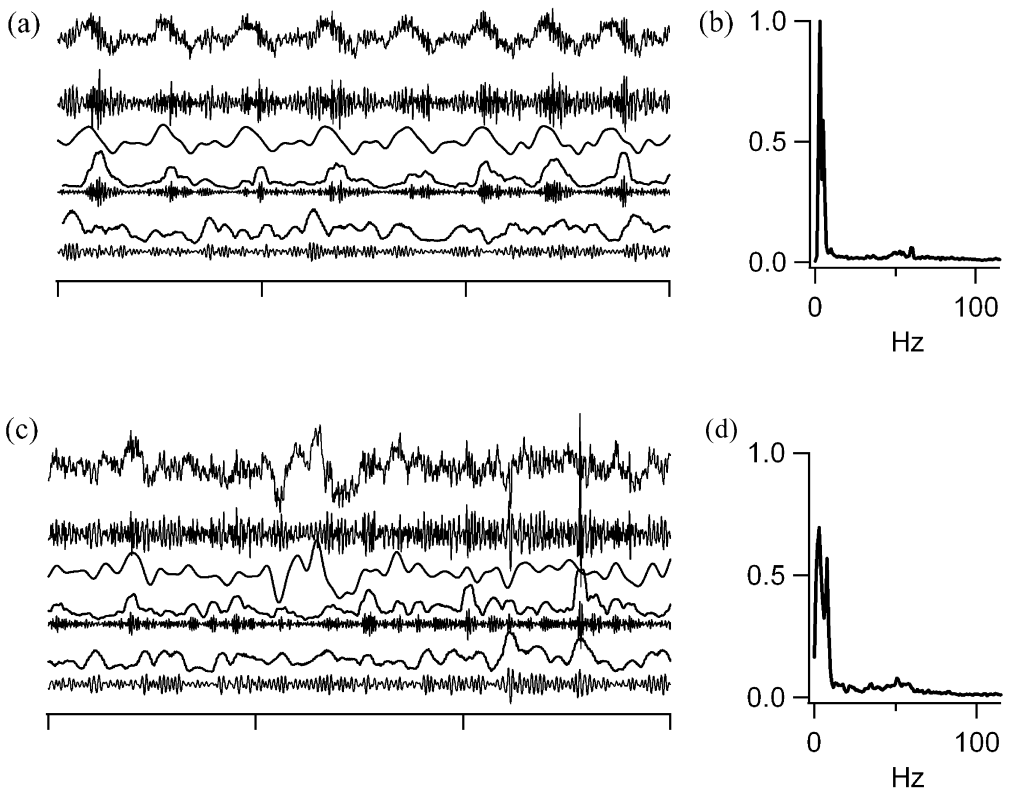

Fig. 4. Mice show high and low frequency gamma oscillations. Data from $\beta 3 +/+$ control animals during immobility (a) and active exploration (c). In both graphs traces are, top to bottom, raw data, 35–115 Hz broadband gamma, theta, smoothed high gamma, high gamma (65–115 Hz), smoothed low gamma, low gamma (35–65 Hz). Data are normalized for ease of display. Power spectra show a small peak in the broad gamma band in both immobility (b) and exploration (d). Three seconds of data are shown in (a) and (c).

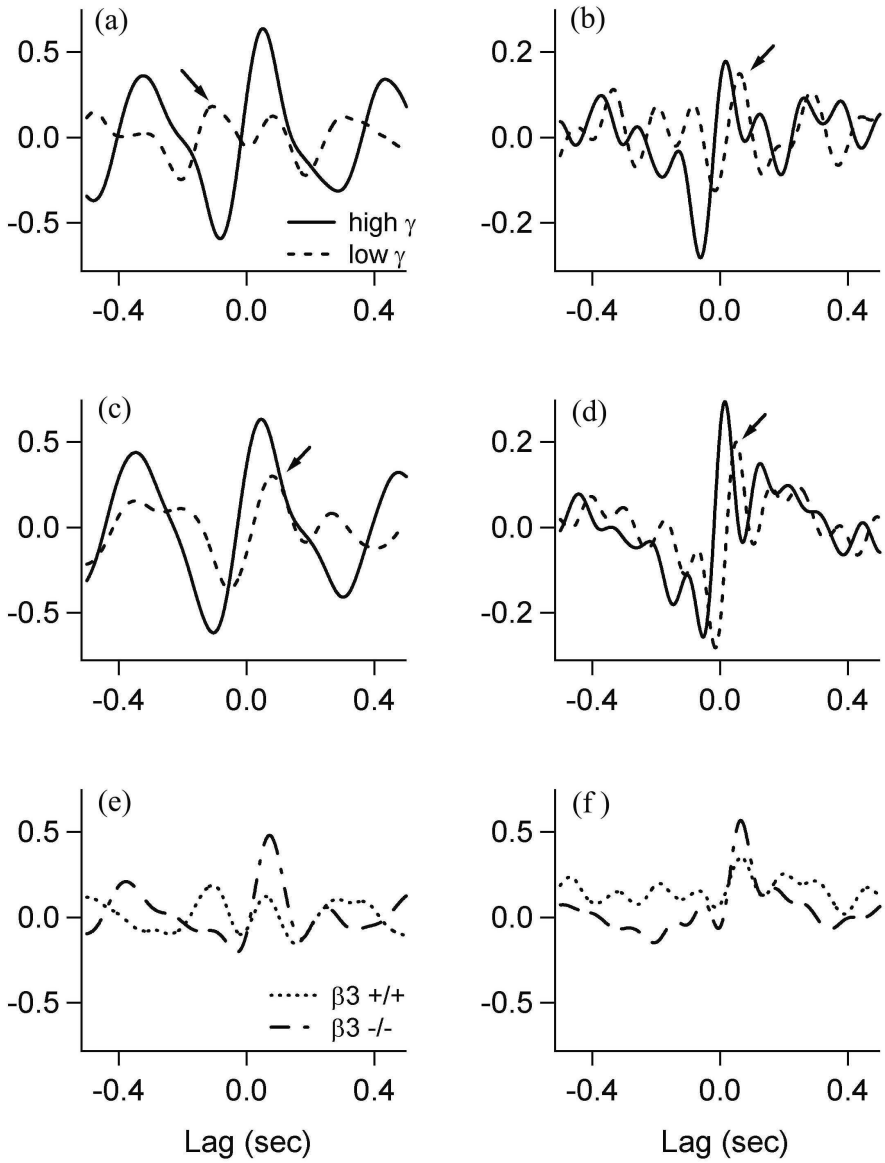

Fig. 5. Correlation patterns between the two gamma bands and theta. (a) Gamma-theta correlations from $\beta 3+/+$ control mice during immobility. Negative lags indicate gamma rhythm leads, positive lags are theta rhythm leads. (b) Gamma-theta correlations from $\beta 3+/+$ mice during exploratory behavior. In $\beta 3+/+$ mice, low frequency gamma has very low correlation with the theta rhythm, while high frequency gamma shows strong correlation during immobility, which is decreased during exploration (b). (c) $\beta 3-/-$ gamma-theta correlation patterns during immobility. Note that the peak of the low gamma-theta correlation (indicated by arrow in a–d) is higher in amplitude than that from $\beta 3+/+$ mice and its peak is just after the high gamma-theta correlation peak. (d) $\beta 3-/-$ gamma-theta correlation patterns during exploratory behavior. Correlations are significantly decreased during exploration. (e) Correlations between smoothed high and low gamma activity during immobility for $\beta 3+/+$ and $\beta 3-/-$ mice. (f) High and low gamma correlations during exploration. Note that $\beta 3-/-$ mice have higher correlation of the two types of oscillations than $\beta 3+/+$ mice. Legend in a is for a–d; legend in e is for e and f.

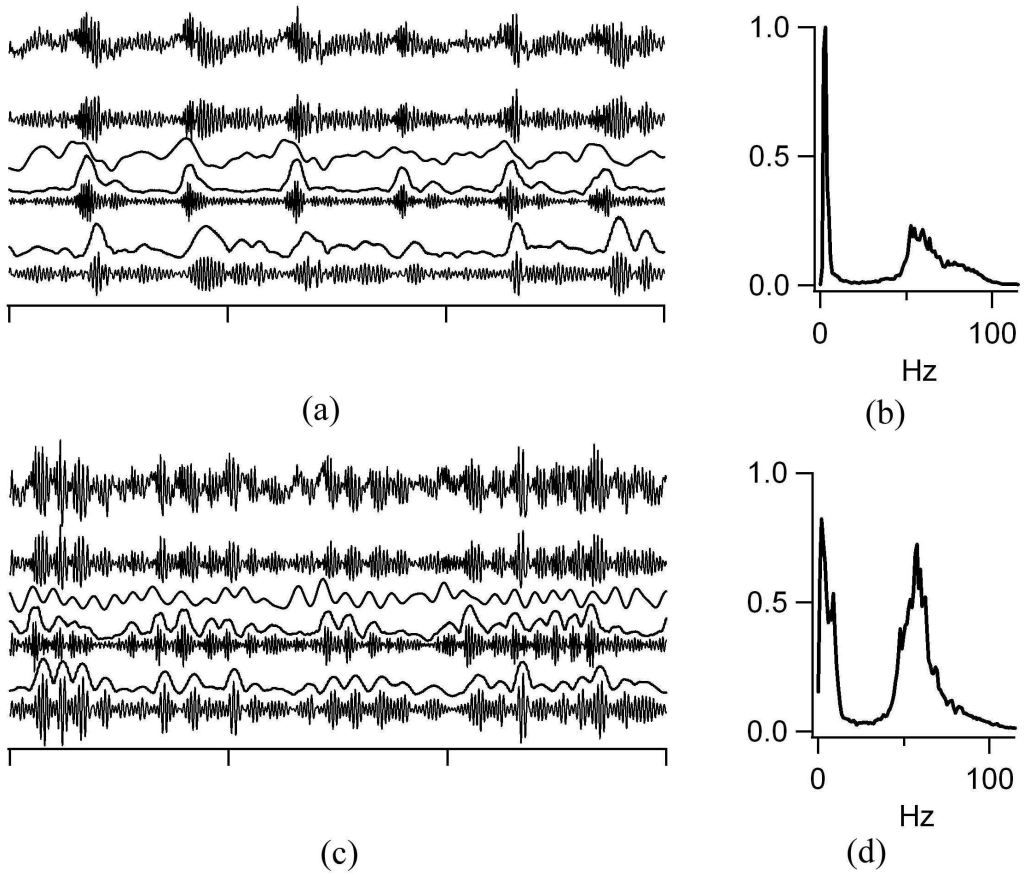

Fig. 6. $\beta 3 -/-$ mice show enhanced gamma activity. Order of traces in a and c is the same as in Fig. 4. (a) Activity during immobility; (b) power spectrum showing peak in the broad gamma band; (c) activity during exploration showing prominent and continuous gamma bursts; (d) power spectrum showing significantly enhance peak in the gamma range. Three seconds of data are shown in (a) and (c).

activity during rest and active exploration similar to that seen in rats (Fig. 4). During immobility the gamma oscillations are pronounced and include large sniff-associated oscillations as well as lower frequency oscillations not associated with inhalation [Figs. 4(a) and (b)]. During exploration, all gamma activity decreases in amplitude and becomes less periodic, similar to that seen in rats [Figs. 4(c) and (d)]. The frequency bands separating the two types of gamma activity and their associations with the OB theta rhythm are similar to those found in rats, 35–65 Hz for low frequency activity and 65–115 Hz for high frequency bursts (Fig. 5). High frequency gamma bursts are associated with inhalation or the peak of the theta oscillation, and low frequency bursts are less or not significantly correlated with the theta oscillation and have an altered phase relationship to it [Fig. 5(a)]. The correlation values are significantly decreased during exploration, and the low gamma activity is similar

to high gamma in reference to the inhalation cycle [Fig. 5(b)]. These patterns were repeated in all four $\beta 3+/+$ mice.

Knockout mice ($\beta 3-/-$) show significantly altered oscillations. During rest, the amplitude of gamma oscillations appears larger but is not significantly increased across animals [Figs. 6(a) and (b)]. During exploration, gamma oscillations are significantly increased in power [Figs. 6(c) and (d)], which was reported earlier [32]. Closer examination of these data shows that the character of gamma oscillations has also changed. During immobility all gamma activity is tightly locked to the inhalation cycle [Fig. 5(c)]. Thus, while there is significant power in the lower part of the gamma band, the activity is not of the type seen in control animals or in rats. Examination of the data during exploration shows that the enhanced gamma rhythm is entirely of the sniff-associated character [Figs. 6(c), (d) and 5(d)]. Correlation between smoothed high and low gamma activity is significantly enhanced in knockout vs. control animals in both behavioral circumstances [Figs. 5(e), (f)]. These patterns were repeated in all three $\beta 3-/-$ mice.

4. Discussion

The traditional picture of olfactory system gamma activity does not make any distinction between parts of the wide gamma band and little distinction between different behavioral and even anesthetized states [9, 16, 21, 27, 28]. While gamma activity is ubiquitous in the mammalian OB and has analogues in the insect system [25, 35], it has thus far been related primarily to odor processing and odor coding. The data reported here show that (1) high frequency gamma activity is associated with the inhalation cycle, (2) during odor sampling and active exploration gamma burst activity is significantly decreased overall relative to the resting state and (3) high amplitude low frequency gamma bursts are relatively uncorrelated with respiration and confined primarily to the resting or motionless state (Figs. 1 and 2). I thus propose classification of gamma activity with analogy to behavioral states associated with type 1 and type 2 theta rhythms in the hippocampus [4], with higher frequency sniff-associated gamma bursts as type 1 gamma and lower frequency sniff-independent gamma bursts associated with alert immobility as type 2 gamma.

Type 1 gamma bursts are likely associated with odor processing, as they can be elicited directly by sniffing an odor and are common during exploratory sniffing (Fig. 3). Previous reports have also shown that type 1 activity is associated with odor processing as a spatial distribution of amplitudes of a common oscillatory waveform over the surface of the OB [13, 15, 16]. This activity is similar to that seen in visual cortex and elsewhere during sensory processing [2, 18]. Type 2 gamma bursts are not significantly or reliably correlated with respiration. In particular, during periods of very high power in alert waiting [Fig. 1(b)], correlation with the theta respiratory wave is often negative [Fig. 2(b)], suggesting that low frequency gamma is inhibited by onset of the inhalation cycle. When high amplitude, low frequency bursts are absent, as during odor identification, type 1 gamma activity expands somewhat into

the lower frequency band, as seen in Fig. 2(c). Visual inspection and power spectral analysis show that the character of this lower frequency activity is markedly different from that seen during alert motionlessness.

While data from knockout animals may be affected by changes elsewhere in the brain and by compensatory changes in the OB during development, data from $\beta 3 -/-$ mice are suggestive of a significant role of granule cell inhibition in OB oscillatory activity. LFP recordings from these mice are deficient in type 2 gamma, even though the power spectrum shows significant gamma band activity in the lower frequency range. Inhibition of granule cells can be from other granule cells or as yet to be identified GABAergic interneurons in the OB, or it may be a result of GABAergic input from other brain regions, such as the nucleus of the diagonal band and elsewhere [37]. The enhanced gamma activity seen in these mice has a relatively strong correlation with theta oscillations, which is different from type 2 gamma defined above and different from activity seen in $\beta 3 +/+$ mice. It is thus probable that in the OB inhibition of granule cells, mediated by $GABA_A$ receptors, drives or is necessary for type 2 gamma oscillations, while type 1 oscillations are produced by the mutual excitatory-inhibitory dendrodendritic synapses between mitral and granule cells as described elsewhere [5]. Therefore, in $\beta 3 -/-$ mice a lack of this inhibition and of type 2 gamma oscillations allows type 1 gamma oscillations to occupy the entire gamma range.

These results show that gamma band dynamics within the OB are dependent on behavioral state and suggest that the oscillations are driven by two sets of synapses within the OB. Production of gamma activity by both mutual inhibition and excitatory-inhibitory interactions is supported by modeling studies [36]. The irregularity seen here during active exploration and odor sniffing is likely facilitated by inhibition of granule cells. When these interactions are absent, gamma activity is pathologically large in amplitude, suggesting abnormal synchrony among mitral cells [32]. A similar phenomenon appears when centrifugal input is temporarily removed [19]. In this case the OB is isolated from the rest of the brain and receives input only from the periphery, producing dramatically enhanced type 1 gamma oscillations, often with a spread of frequency into the lower part of the gamma band. Because centrifugal input arrives largely onto the basal dendrites of granule cells, it is likely that one of its effects is either to enhance putative mutual inhibition via excitatory input to the granule cells or to inhibit the granule cells via direct GABAergic input.

What then are the functional roles of type 1 and type 2 gamma oscillations? Nearly periodic oscillations are often an indicator of underlying synchronous or correlated firing in large numbers of cells with similar phase relationships to the oscillatory frequency measured at the population level [9, 19, 35]. Inhibitory drive to granule cells has been proposed here and earlier as a desynchronizing force in OB dynamics [32]. However, during alert waiting these connections may also generate high amplitude, nearly periodic type 2 bursts, suggesting that they are also

capable of synchronizing OB activity in specific behavioral circumstances. These bursts are similar to attention related gamma bursts in the somatomotor system and may be a ubiquitous phenomenon associated with this cognitive-motor state [8, 31]. Type 1 oscillations are more periodic during spontaneous exploration of a novel environment, and during fast sniffing associated with odor discrimination they are relatively aperiodic. During these fast sniffing epochs mitral cells in the OB uncouple from respiratory driving [24], suggesting that mitral cell desynchronization, as represented by aperiodic broadband type 1 gamma, is part of odor discrimination and that this desynchronization may be further facilitated by the increase in respiratory frequency.

In conclusion, gamma oscillations are not of a single type associated with odor coding in the OB. They are of at least two types, distinguishable by their differential relationships to behavioral state and the sniff cycle and by their frequency characteristics. These two rhythms are likely produced by different synaptic interactions in the OB. In some animals or behavioral conditions the frequency bands may overlap, in which case the behavioral and sniff-cycle criteria are the defining characteristics. Type 1 gamma is likely an indicator of odor processing, whether it is of enhanced or diminished periodicity, while prominent type 2 gamma indicates an alert cognitive state, as it is strongest and most reliable during alert immobility with low respiratory rates in trained animals.

Acknowledgments

All animal procedures were done in accordance with and oversight by the Animal Care and Use Committees at UC Berkeley, UCLA and the University of Chicago and conformed to NIH and AAALAC guidelines. I thank Zachary Haga and Catherine Lowry for data for some of the figures, Hugh Gibbons for assistance in animal care and Maryellen Begley for technical support. I also thank Nancy Kopell for enlightening discussions, Walter Freeman, in whose laboratory some of the behavioral recordings were done (NIMH grant MH06686), Istvan Mody, in whose laboratory the $\beta 3$ mice were studied along with Zoltan Nusser (NINDS grant NS 35985), and Gregg Homanics for the initial breeding pairs for the UCLA $\beta 3 -/-$ colony. This work was supported by a grant to LK from the University of Chicago Brain Research Fund.

References

[1] Adrian E. D., Olfactory reactions in the brain of the hedgehog, *J. Physiol.* **100** (1942) pp. 459–473.

[2] Barrie J. M., Freeman W. J. and Lenhart M. D., Spatiotemporal analysis of prepyriform, visual, auditory, and somesthetic surface eegs in trained rabbits, *J. Neurophysiol.* **76** (1996) pp. 520–539.

[3] Bazhenov M., Stopfer M., Rabinovich M., Huerta R., Abarbanel H. D. I., Sejnowski T. J. and Laurent G., Model of transient oscillatory synchronization in the locust antennal lobe, *Neuron* **30** (2001) pp. 553–567.

[4] Bland B. H., Seto M. G., Sinclair B. R. and Fraser S. M., The pharmacology of hippocampal theta cells: Evidence that the sensory processing correlate is cholinergic, *Brain Res.* **299** (1984) pp. 121–131.

[5] Bressler S. L. and Freeman W. J., Frequency analysis of olfactory system EEG in cat, rabbit, and rat, *Electroencephalogr. Clin. Neurophysiol.* **50** (1980) pp. 19–24.

[6] Chrobak J. J., Lorincz A. and Buzsaki G., Physiological patterns in the hippocampo-entorhinal cortex system, *Hippocampus* **10** (2000) pp. 457–465.

[7] Csicsvari J., Jamieson B., Wise K. D. and Buzsaki G., Mechanisms of gamma oscillations in the hippocampus of the behaving rat, *Neuron* **37** (2003) pp. 311–322.

[8] Donoghue J. P., Sanes J. N., Hatsopoulos N. G. and Gaal G., Neural discharge and local field potential oscillations in primate motor cortex during voluntary movements, *J. Neurophysiol.* **79** (1998) pp. 159–173.

[9] Eeckman F. H. and Freeman W. J., Correlations between unit firing and EEG in the rat olfactory system, *Brain Res.* **528** (1990) pp. 238–244.

[10] Engel A. K., Konig P., Gray C. M. and Singer W., Stimulus-dependent neuronal oscillations in cat visual cortex: Inter-columnar interaction as determined by cross-correlation analysis, *Eur. J. Neurosci.* **2** (1990) pp. 588–606.

[11] Erdi P., Aradi I. and Grobler T., Rhythmogenesis in single cells and population models: Olfactory bulb and hippocampus, *Biosystems* **40** (1997) pp. 45–53.

[12] Freeman W. J., *Mass Action in the Nervous System* (Academic Press, New York, 1975).

[13] Freeman W. J., Spatial properties of an EEG event in the olfactory bulb and cortex, *Electroencephalogr. Clin. Neurophysiol.* **44** (1978) pp. 586–605.

[14] Freeman W. J., Simulation of chaotic EEG patterns with a dynamic model of the olfactory system, *Biol. Cybern.* **56** (1987) pp. 139–150.

[15] Freeman W. J. and Schneider W., Changes in spatial patterns of rabbit olfactory EEG with conditioning to odors, *Psychophysiology* **19** (1982) pp. 44–56.

[16] Freeman W. J. and Viana Di Prisco G., Relation of olfactory EEG to behavior: Time series analysis, *Behav. Neurosci.* **100** (1986) pp. 753–763.

[17] Friedrich R. W. and Laurent G., Dynamic optimization of odor representations by slow temporal patterning of mitral cell activity, *Science* **291** (2001) pp. 889–894.

[18] Gray C. M., Engel A. K., Konig P. and Singer W., Stimulus-dependent neuronal oscillations in cat visual cortex: Receptive field properties and feature dependence, *Eur. J. Neurosci.* **2** (1990) pp. 607–619.

[19] Gray C. M. and Skinner J. E., Centrifugal regulation of neuronal activity in the olfactory bulb of the waking rabbit as revealed by reversible cryogenic blockade, *Exp. Brain Res.* **69** (1988) pp. 378–386.

[20] Homanics G. E., DeLorey T. M., Firestone L. L., Quinlan J. J., Handforth A., Harrison N. L., Krasowski M. D., Rick C. E., Korpi E. R., Makela R., Brilliant M. H., Hagiwara N., Ferguson C., Snyder K. and Olsen R. W., Mice devoid of gamma-aminobutyrate type a receptor beta3 subunit have epilepsy, cleft palate, and hypersensitive behavior, *Proc. Natl. Acad. Sci. USA* **94** (1997) pp. 4143–4418.

[21] Kashiwadani H., Sasaki Y. F., Uchida N. and Mori K., Synchronized oscillatory discharges of mitral/tufted cells with different molecular receptive ranges in the rabbit olfactory bulb, *J. Neurophysiol.* **82** (1999) pp. 1786–1792.

[22] Kay L. M. and Freeman W. J., Bidirectional processing in the olfactory-limbic axis during olfactory behavior, *Behav. Neurosci.* **112** (1998) pp. 541–553.

[23] Kay L. M., Lancaster L. R. and Freeman W. J., Reafference and attractors in the olfactory system during odor recognition, *Int. J. Neural Syst.* **7** (1996) pp. 489–495.

[24] Kay L. M. and Laurent G., Odor- and context-dependent modulation of mitral cell activity in behaving rats, *Nature Neurosci.* **2** (1999) pp. 1003–1009.

[25] Laurent G. and Davidowitz H., Encoding of olfactory information with oscillating neural assemblies, *Science* **265** (1994) pp. 1872–1875.

[26] Leung L. S., Generation of theta and gamma rhythms in the hippocampus, *Neurosci. Biobehav. Rev.* **22** (1998) pp. 275–290.

[27] Li Z. and Hopfield J. J., Modeling the olfactory bulb and its neural oscillatory processings, *Biol. Cybern.* **61** (1989) pp. 379–392.

[28] Linster C. and Hasselmo M., Modulation of inhibition in a model of olfactory bulb reduces overlap in the neural representation of olfactory stimuli, *Behav. Brain Res.* **84** (1997) pp. 117–127.

[29] Maldonado P. E., Friedman-Hill S. and Gray C. M., Dynamics of striate cortical activity in the alert macaque: II. Fast time scale synchronization, *Cereb. Cortex* **10** (2000) pp. 1117–1131.

[30] Murthy V. N. and Fetz E. E., Coherent 25- to 35-hz oscillations in the sensorimotor cortex of awake behaving monkeys, *Proc. Natl. Acad. Sci. USA* **89** (1992) pp. 5670–5674.

[31] Murthy V. N. and Fetz E. E., Oscillatory activity in sensorimotor cortex of awake monkeys: Synchronization of local field potentials and relation to behavior, *J. Neurophysiol.* **76** (1996) pp. 3949–3967.

[32] Nusser Z., Kay L. M., Laurent G., Homanics G. E. and Mody I., Disruption of GABA(A) receptors on GABAergic interneurons leads to increased oscillatory power in the olfactory bulb network, *J. Neurophysiol.* **86** (2001) pp. 2823–2833.

[33] Sokal R. R. and Rohlf F. J., *Biometry* (W. H. Freeman and Co., New York, 1995).

[34] Stopfer M., Bhagavan S., Smith B. H. and Laurent G., Impaired odour discrimination on desynchronization of odour- encoding neural assemblies, *Nature* **390** (1997) pp. 70–74.

[35] Wehr M. and Laurent G., Odour encoding by temporal sequences of firing in oscillating neural assemblies, *Nature* **384** (1996) pp. 162–166.

[36] Whittington M. A., Traub R. D., Kopell N., Ermentrout B. and Buhl E. H., Inhibition-based rhythms: Experimental and mathematical observations on network dynamics, *Int. J. Psychophysiol.* **38** (2000) pp. 315–336.

[37] Zaborszky L., Carlsen J., Brashear H. R. and Heimer L., Cholinergic and GABAergic afferents to the olfactory bulb in the rat with special emphasis on the projection neurons in the nucleus of the horizontal limb of the diagonal band, *J. Comp. Neurol.* **243** (1986) pp. 488–509.